

## Article

# A role for the Tgf- $\beta$ /Bmp co-receptor Endoglin in the molecular oscillator that regulates the hair follicle cycle

María I. Calvo-Sánchez<sup>1,2,6</sup>, Sandra Fernández-Martos<sup>6</sup>, Elisa Carrasco<sup>1</sup>, Gema Moreno-Bueno<sup>1,3</sup>, Carmelo Bernabéu<sup>4</sup>, Miguel Quintanilla<sup>1</sup>, and Jesús Espada<sup>1,5,6,\*</sup>

<sup>1</sup> Instituto de Investigaciones Biomédicas ‘Alberto Sols’, Consejo Superior de Investigaciones Científicas (CSIC)-Departamento de Bioquímica, Universidad Autónoma de Madrid (UAM), Madrid 28029, Spain

<sup>2</sup> Instituto de Investigaciones Biosanitarias, Facultad de Ciencias Experimentales, Universidad Francisco de Vitoria (UFV), Pozuelo de Alarcón 28223, Spain

<sup>3</sup> Centro de Investigación Biomédica en Red de Cáncer (CIBERONC), Spain

<sup>4</sup> Centro de Investigaciones Biológicas, Consejo Superior de Investigaciones Científicas (CSIC) and Centro de Investigación Biomédica en Red de Enfermedades Raras (CIBERER), Madrid 28040, Spain

<sup>5</sup> Centro Integrativo de Biología y Química Aplicada, Universidad Bernardo O’Higgins, Santiago 8370854, Chile

<sup>6</sup> Present address: Instituto Ramón y Cajal de Investigación Sanitaria (IRYCIS), Hospital Universitario Ramón y Cajal, Madrid, Spain

\* Correspondence to: Jesús Espada, E-mail: jespada1968@gmail.com

Edited by Anming Meng

The hair follicle is a biological oscillator that alternates growth, regression, and rest phases driven by the sequential activation of the proliferation/differentiation programs of resident stem cell populations. The activation of hair follicle stem cell niches and subsequent entry into the growing phase is mainly regulated by Wnt/ $\beta$ -catenin signalling, while regression and resting phases are mainly regulated by Tgf- $\beta$ /Bmp/Smad activity. A major question still unresolved is the nature of the molecular switch that dictates the coordinated transition between both signalling pathways. Here we have focused on the role of Endoglin (Eng), a key co-receptor for members of the Tgf- $\beta$ /Bmp family of growth factors. Using an *Eng* haploinsufficient mouse model, we report that *Eng* is required to maintain a correct follicle cycling pattern and for an adequate stimulation of hair follicle stem cell niches. We further report that  $\beta$ -catenin binds to the *Eng* promoter depending on Bmp signalling. Moreover, we show that  $\beta$ -catenin interacts with Smad4 in a Bmp/Eng-dependent context and both proteins act synergistically to activate *Eng* promoter transcription. These observations point to the existence of a growth/rest switching mechanism in the hair follicle that is based on an Eng-dependent feedback cross-talk between Wnt/ $\beta$ -catenin and Bmp/Smad signals.

**Keywords:** Endoglin, hair follicle, skin stem cells, Wnt/ $\beta$ -catenin, Tgf- $\beta$ /Bmp/Smad

## Introduction

The hair follicle can be considered as a complex mini-organ with a distinctive morpho/functional identity that continuously cycles through growing (anagen), regression (catagen), and resting (telogen) phases (Mu et al., 2001; Fuchs, 2007; Plikus et al., 2008; Schneider et al., 2009; Hsu et al., 2014). The activity of the whole hair follicle is controlled by specialized populations of

stem cells mainly located in the bulge region, site of insertion of the arrector pili muscle, and in a morphologically distinguishable structure below the bulge known as the hair germ (Cotsarelis et al., 1990; Sun et al., 1991; Morris et al., 2004; Tumber et al., 2004; Greco et al., 2009; Rompolas et al., 2013; Hsu et al., 2014). Hair follicle stem cells periodically leave their quiescent state and are induced to proliferate, expand, and differentiate in response to oscillating signals originated in the surrounding niche (Fuchs, 2007; Plikus et al., 2008; Hsu et al., 2014). At the onset of the anagen phase, hair germ stem cells are the first to proliferate giving rise to a transit amplifying population of progenitor cells that migrate downwards ultimately forming the hair matrix region. Matrix cells can in turn proliferate and differentiate upwards giving rise to the hair shaft and the surrounding inner root sheath. Bulge stem cells give rise to the outer root sheath, a cell population retaining

Received February 21, 2018. Revised August 3, 2018. Accepted September 18, 2018.

© The Author(s) (2018). Published by Oxford University Press on behalf of Journal of Molecular Cell Biology, IBCB, SIBS, CAS.

This is an Open Access article distributed under the terms of the Creative Commons Attribution Non-Commercial License (<http://creativecommons.org/licenses/by-nc/4.0/>), which permits non-commercial re-use, distribution, and reproduction in any medium, provided the original work is properly cited. For commercial re-use, please contact [journals.permissions@oup.com](mailto:journals.permissions@oup.com)

stemness characteristics that envelops the matrix transit amplifying cell population at the differentiating core of the hair follicle (Hsu et al., 2014). Once matrix cells stop their proliferation and differentiation programs, hair follicle enters in the catagen phase and its lower part undergoes a rapid involution triggered by the activation of matrix cell apoptosis. Eventually, the lower part of the hair follicle is reduced to a single epithelial strand, bringing the dermal papilla into close proximity to the bulge region (Schneider et al., 2009). This process is followed by the entry of the hair follicle in the resting or telogen phase, where dermal papilla cells become progressively competent to activate again the bulge region in response to specific signals. The cyclic nature of hair follicle activity, and the fact that this activity depends on a well-defined population of stem cells, makes this structure a suitable biological model to investigate new modes of functional regulation of adult stem cell dynamic micro-environments in mammals.

Different paracrine signalling pathways have been directly involved in the regulation of the hair follicle growth cycle (Plikus et al., 2008). Among them, Wnt/ $\beta$ -catenin and Bmp/Smad are the best characterized to date (Supplementary Figure S1). Wnt/ $\beta$ -catenin signalling regulates the onset and progression of the anagen (Schneider et al., 2009; Shimomura and Christiano, 2010), while activation of Bmp/Smad signalling during mid anagen is involved in the entrance of the hair follicle in the catagen and telogen states (Plikus and Chuong, 2008; Plikus et al., 2008; Oshimori and Fuchs, 2012). The activation of the Bmp/Smad pathway is currently used to determine the hair follicle stages, using the expression levels of Bmp2 and Bmp4 as late anagen and refractory telogen markers (Plikus et al., 2008). Progressive activation of Bmp/Smad signalling in an out-of-phase pattern with respect to Wnt/ $\beta$ -catenin signalling further divides the telogen into two sub-phases, refractory (expression of Bmp) and competent (absence of Bmp) (Plikus et al., 2008) (Supplementary Figure S1). During the refractory telogen, hair follicles are unable to respond to anagen re-entry stimulation even in the presence of Wnt/ $\beta$ -catenin signalling. Throughout the second part of the telogen phase, attenuated Bmp signalling allows the anagen re-entry wave to propagate and hair follicles are competent to respond to Wnt/ $\beta$ -catenin signalling. The whole system can be accurately described as a biological oscillator regulated by negative feedback mechanisms (Sasai, 2013) in which two broadly defined interacting cell populations, bulge stem cells and dermal papilla niche cells, alternate active and inactive states depending on a basic stimulatory signal (Wnt/ $\beta$ -catenin) that is cyclically regulated by a negative signal (Bmp/Smad). On the other hand, taking into account that the activation of the Wnt pathway strengthens Bmp signalling (Baik et al., 2016), a major unanswered question is the nature of the molecular mechanisms that so precisely regulate the coordinated switch between growth and rest, and backwards, in the hair follicle stem cell niche.

Here we have focused on the role of Endoglin (Eng), an essential co-receptor of Bmp growth factors, in the regulation of the hair follicle cycle. In the mouse, *Eng* is expressed early during embryonic development on mesenchymal tissue derived from

the endocardium and also in the vascular endothelium, playing a critical role in cardiovascular system development and homeostasis (Bourdeau et al., 1999). After birth, *Eng* is expressed mainly in endothelial cells, and, to a lesser degree, in macrophages, fibroblasts, vasculature muscle cells, mesenchymal and haematopoietic stem cells, blood cells, and also in several regions of the skin, such as the interfollicular epithelium (IFE), hair follicles, and the dermis (Quintanilla et al., 2003; Supplementary Figure S2). Mutations in *Eng* gene are associated to the hereditary haemorrhagic telangiectasia vascular dysplasia, termed HHT1 (McAllister et al., 1994; López-Novoa and Bernabeu, 2010; Kapur et al., 2013). *Eng* is also involved in skin regeneration during wound healing (Pérez-Gómez et al., 2014) and can suppress keratinocyte proliferation in early stages of a multistage mouse skin carcinogenesis model, driving malignant progression, invasion and metastasis, in later phases (Quintanilla et al., 2003; Pérez-Gómez et al., 2007). These observations point to important roles for *Eng* in the regulation of skin stem cell niches and in the maintenance of skin homeostasis similar to the role of this protein in the haematopoietic system (Baik et al., 2016).

## Results

### *Eng shows a hair follicle cycle-dependent expression pattern in mouse skin that is deregulated in Eng haploinsufficient mice*

We first sought to determine the expression pattern of *Eng* during the hair follicle cycle in wild-type (*Eng*<sup>+/+</sup>) C57Bl/6 mice, using as experimental framework the second of the two coordinated hair follicle cycles that take place in this biological model. This second cycle, ranging from postnatal days 30 to 100, is more lengthy and easily manageable from an experimental perspective. We found that the *Eng* mRNA exhibited a hair cycle-dependent expression pattern in *Eng*<sup>+/+</sup> mice, showing a very low expression level during the anagen phase, a gradual increase, starting at the onset of the telogen (postnatal day 50, anagen/refractory telogen transition), to reach a maximum peak at the competent telogen/propagant anagen transition (postnatal day 90), followed by a drastic decrease henceforth (Figure 1A). This result was broadly confirmed by the analysis of the *Eng* protein expression and localization pattern in the skin (Figure 1B and Supplementary Figure S2). Interestingly, such expression pattern perfectly fits with the profile of master feedback target regulators of the hair follicle cycle predicted by a robust mathematical model that describes hair follicle dynamics as the result of coupled mesenchymal and epithelial oscillators, and that, in fact, identifies *Eng* as one of those potential targets (Tasseff et al., 2014).

These observations prompted us to investigate the effect of a functional decrease of *Eng* in the skin. To this end, we used C57Bl/6 mice lacking a copy of the *Eng* gene (*Eng*<sup>+/-</sup>). Haploinsufficient *Eng*<sup>+/-</sup> mice in a C57Bl/6 background are essentially equivalent to wild-type animals with respect to physiopathology, behaviour, fertility, and life expectancy. Clinical signs of HHT are almost absent in these animals (Bourdeau et al., 1999; Quintanilla et al., 2003). Moreover, the *Eng*<sup>+/-</sup> model also ensured the effective and functional reduction of *Eng* in the tissue. As expected, *Eng*<sup>+/-</sup> mice showed a drastic reduction

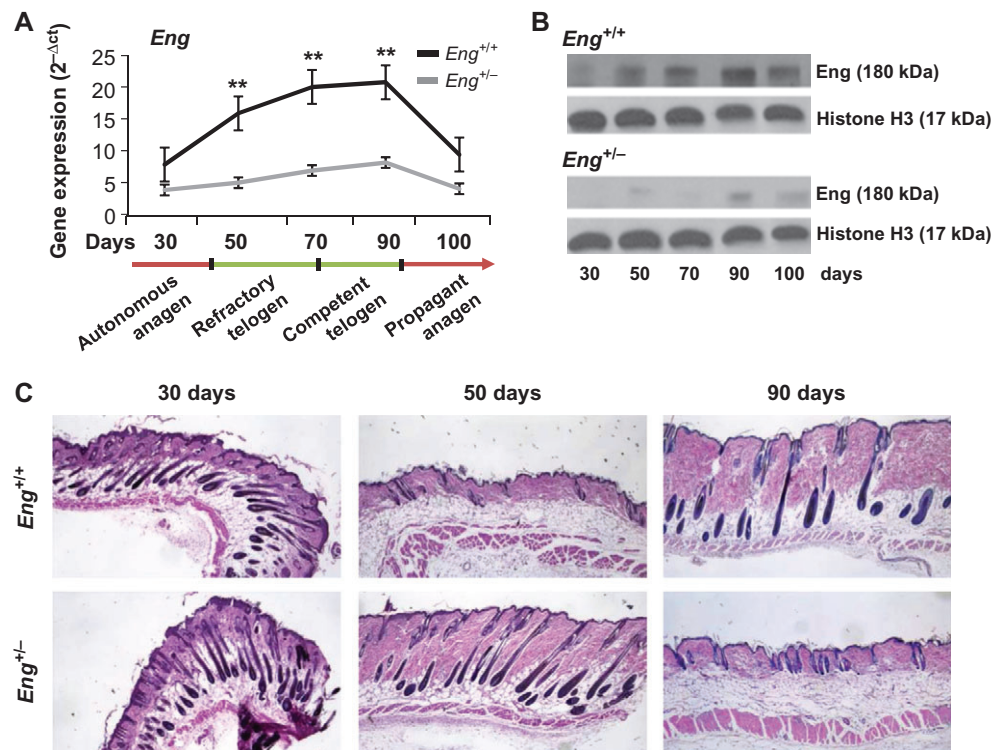


**Figure 1** The *Eng* cyclic expression pattern in mouse skin is deregulated under *Eng* haploinsufficiency resulting in a delayed entry into the refractory telogen phase. (A) *Eng* mRNA expression quantification by qRT-PCR, normalized to 18S rRNA, in *Eng*<sup>+/+</sup> and *Eng*<sup>+/-</sup> mouse dorsal skin at different time points (postnatal days) of the hair growth cycle, showing the hair follicle growth phase-dependent cyclic expression pattern of this gene. The mean ± SE was represented (n = 3 in each time point). (B) Immunoblot analysis of *Eng* protein expression, with histone H3 as a loading control, in *Eng*<sup>+/+</sup> and *Eng*<sup>+/-</sup> mouse dorsal skin at the indicated time points (postnatal days) during the hair follicle cycle. (C) Morphology of *Eng*<sup>+/+</sup> and *Eng*<sup>+/-</sup> mouse dorsal skin at the indicated time points (postnatal days) showing hair follicles in full-length vertical orientation in histological sections stained with haematoxylin–eosin. A significantly delayed entry into the refractory telogen (postnatal day 50) is observed in *Eng*<sup>+/-</sup> animals. Black bars represent average hair follicle length in each time point.

of *Eng* expression in the skin and a concomitant loss of a cyclic patterning during the hair follicle cycle (Figure 1A and B; Supplementary Figure S2). Although no differences were observed in hair follicle formation and dynamics during early postnatal development, a striking delay in the onset of the second telogen phase (postnatal day 50 in wild-type animals) and in the entry of the subsequent anagen phase was observed in *Eng*<sup>+/-</sup> mice as compared to control *Eng*<sup>+/+</sup> littermates (Figure 1C). The altered pattern was maintained through all the second telogen phase so that *Eng*<sup>+/+</sup> mice entered in the subsequent anagen phase by Day 90 while *Eng*<sup>+/-</sup> littermates were still in telogen (Figure 1C). There was no defined temporal pattern of entrance into the second anagen in *Eng*<sup>+/-</sup> hair follicles. This behaviour is probably influenced by the fact that, in the C57Bl/6 experimental model, from postnatal days ~90–100 onwards, there is no more synchronicity in the hair follicle growth cycle. As *Eng*<sup>+/-</sup> mice present a delayed response to anagen entry in the second hair follicle growth cycle, the re-entry into the next growing phase occurs randomly beyond this point. Such unusually modified hair follicle cycling was consistently observed in 97% of the analysed animals (n = 50).

Interestingly, no significant increase in the number of apoptotic cells was found in the hair follicles of *Eng*<sup>+/-</sup> animals (Supplementary Figure S3). Actually, a very low number of apoptotic cells were detected in the skin of *Eng*<sup>+/+</sup> and *Eng*<sup>+/-</sup> animals, a result consistent with the fact that in the C57Bl/6 mouse model the catagen phase is very rapid and last for only 2–3 days (Paus et al., 1999). This result suggests that *Eng* plays a central role in the regulation of telogen entry, as predicted for feedback target regulators in the coupled dual oscillator model of hair follicle dynamics (Tasseff et al., 2014).

#### The molecular signals that dictate the anagen–telogen transition are out-of-phase in *Eng* haploinsufficient mice

As *Eng* is a co-receptor of the Bmp cytokine family and, particularly Bmp4 is directly involved in the regulation of telogen entry, being used as a marker of late anagen and refractory telogen (Plikus et al., 2008), we investigated the expression pattern of this gene during the hair follicle cycle in *Eng*<sup>+/-</sup> mice as compared to control *Eng*<sup>+/+</sup> littermates. As expected, in wild-type animals, Bmp4 showed high expression levels in the late anagen/refractory telogen transition that gradually decreased with

progression through the hair follicle cycle and this pattern was not significantly altered in haploinsufficient conditions (Figure 2A) indicating that the background pattern of molecular inputs that define the entry/exit of the hair follicle into different growth phases is not altered in *Eng* haploinsufficient conditions. We further analysed the expression pattern of *Id1*, a transcriptional target of *Bmp4* signalling in the skin (Ahmed et al., 2011). Interestingly, we found that *Id1* showed an expression pattern resembling the profile of *Bmp4* in *Eng*<sup>+/+</sup> animals, but this pattern was completely abrogated in *Eng*<sup>+/-</sup> littermates (Figure 2A).

In addition, we analysed the expression pattern of *Wnt3a* and two gene targets of Wnt signalling in the skin, *Jagged* and *Ovol1*. The results showed no significant differences in the expression pattern of these targets between *Eng*<sup>+/+</sup> and *Eng*<sup>+/-</sup> animals, suggesting that *Eng* haploinsufficiency does not affect Wnt signalling. As a whole, these results indicate that *Eng* is directly involved in the transmission of Bmp, but not Wnt, signals in the skin.

Next, we wondered if the defective transmission of Bmp signals in *Eng*<sup>+/-</sup> animals may disturb the molecular framework that

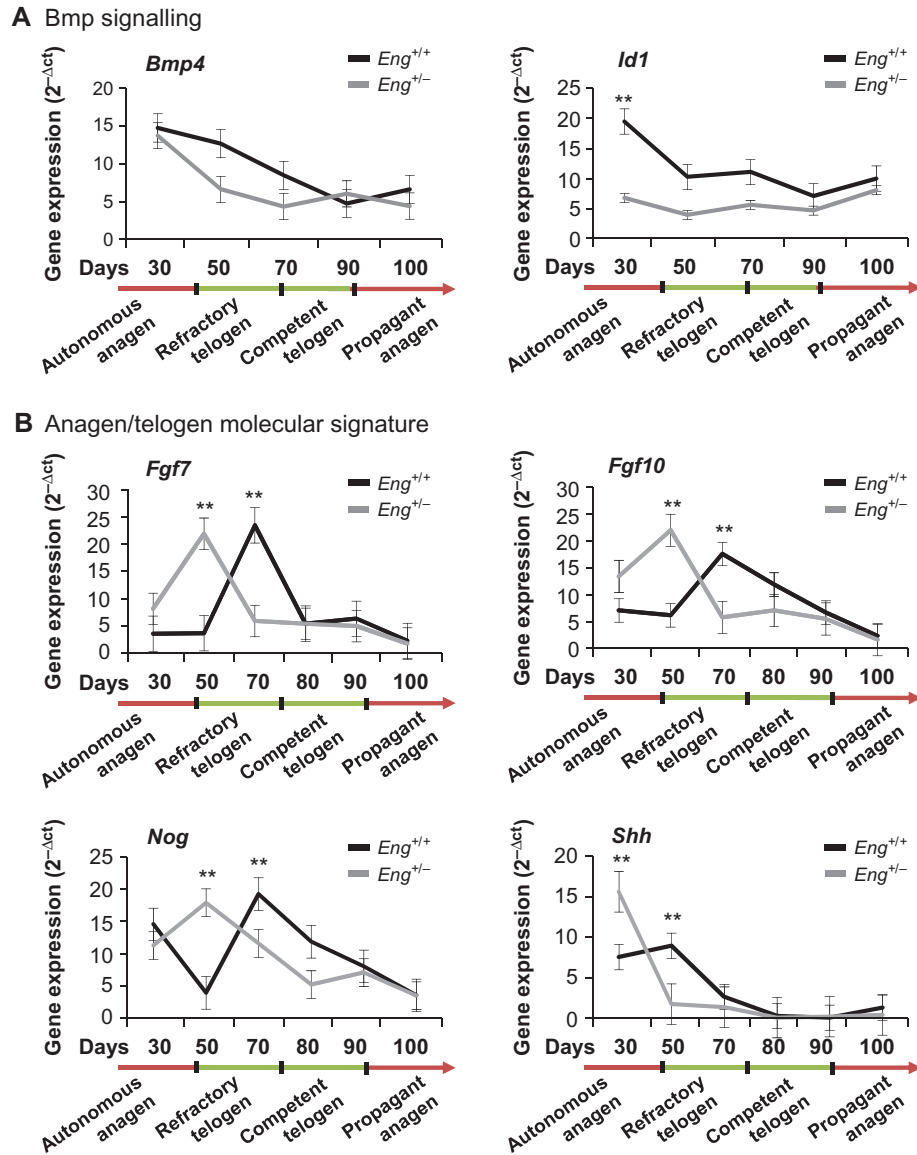


**Figure 2** Disruption of Bmp signalling in the skin is associated with a premature out-of-phase expression of factors implicated in the regulation of hair follicle phase transitions in *Eng* haploinsufficient mice. (A) *Bmp4* and *Id1* mRNA expression in *Eng*<sup>+/+</sup> and *Eng*<sup>+/-</sup> mouse dorsal skin at different points of the hair growth cycle, showing the loss of cyclic expression pattern of *Id1*, but not *Bmp4*, in *Eng*<sup>+/-</sup> animals. (B) *Fgf7*, *Fgf10*, *Noggin*, and *Shh* mRNA expression in *Eng*<sup>+/+</sup> and *Eng*<sup>+/-</sup> mouse dorsal skin at different points of the hair growth cycle, showing the premature out-of-phase expression of all these factors in *Eng*<sup>+/-</sup> animals during autonomous anagen/refractory telogen transition. In all cases, gene expression was quantified by qRT-PCR, normalized to 18S rRNA, and the mean  $\pm$  SE was represented; \* $P$  < 0.01, \*\* $P$  < 0.005 ( $n$   $\geq$  3 in each time point).



modulates anagen/telogen/anagen transitions. To this end, we investigated the gene expression patterns of key factors required to induce the re-entry of the hair follicle into the growing phase, including Fgf7, Fgf10, Nogging, and Shh (Hsu et al., 2014 and references therein). Notably, we found that all these factors recurrently showed a delayed out-of-phase expression pattern in  $Eng^{+/-}$  mice as compared to control  $Eng^{+/+}$  littermates (Figure 2B). This result is consistent with the deregulated hair follicle cycling pattern observed in these animals (Figure 1C) and suggests that  $Eng$  haploinsufficiency impairs the molecular oscillator that dictates the alternation of Wnt/ $\beta$ -catenin and Bmp/Tgf- $\beta$ /Smad signalling that occurs during the hair follicle cycle.

*Eng is required for correct telogen entry/exit timing during the hair follicle cycle*

Our results suggest that  $Eng$  plays important roles in the anagen/refractory telogen and competent telogen/anagen transitions during the hair growth cycle. In this context, we hypothesized that a physiological stimulus to activate hair growth in the anagen/refractory telogen transition (postnatal day 50), when the hair follicle is unable to respond in normal conditions to stimulatory signals, or in the competent telogen/anagen transition (postnatal day 90), when the hair follicle is now ready

to respond to growth signals (Plikus et al., 2008; Plikus, 2009), should have different responses in  $Eng^{+/+}$  and  $Eng^{+/-}$  littermates.

To test this hypothesis, we performed a series of hair clipping experiments in the back skin of sample animals at 50 or 90 days after birth. As expected by the high expression of Bmp4, clipping stimulation in wild-type animals resulted in a delayed response of hair follicle growth during the anagen/refractory telogen transition, as compared to the rapid induction observed during the competent telogen/anagen transition (Figure 3A), coinciding with low expression of Bmp4 and according to the molecular background of the effectors in the tissue in each time point. Thus, these animals showed a strong activation of Bmp/Smad signalling and a corresponding attenuation of Wnt/ $\beta$ -catenin signalling at Day 50, but a reversed signature at Day 90 (Supplementary Figure S5). By sharp contrast, this standard scenario was completely altered in  $Eng$  haploinsufficient animals. After clipping stimulation,  $Eng^{+/-}$  littermates showed continuous hair growth during the refractory telogen, despite being defined by high Bmp4 expression, but a significant delayed response during the competent telogen (Figure 3B), marked by lower Bmp4 expression, a situation mirrored by an altered molecular background signature of the effectors in each time point (Supplementary Figure S5). These results are in agreement with a defective transmission of the Bmp/Smad signal in  $Eng^{+/-}$  animals.

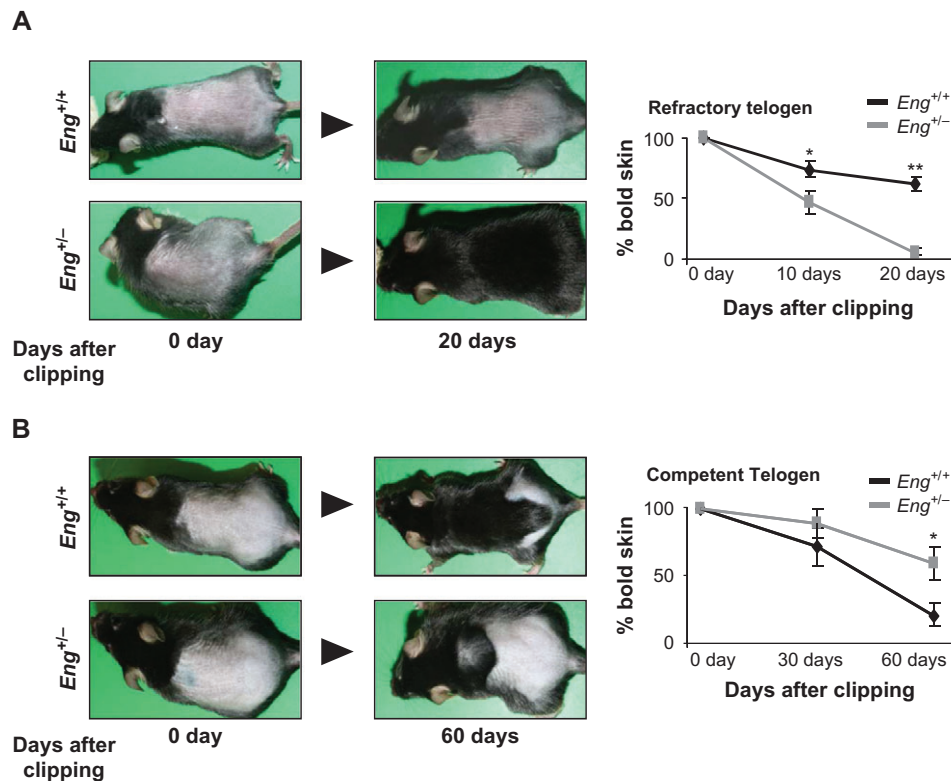


**Figure 3** Hair growth is strongly accelerated during the refractory telogen but is significantly delayed during the competent telogen in  $Eng$  haploinsufficient mice after clipping stimulation. (A and B) Induction of hair growth after dorsal hair clipping in  $Eng^{+/+}$  and  $Eng^{+/-}$  mice during the anagen/refractory telogen transition (postnatal day 50) (A) or the competent telogen phase (postnatal day 90) (B). The experiment finished when most animals of one genotype showed fully completed hair re-growth in the clipped area. Images are representative of three independent experiments including at least three mice for each genotype. The mean percentage of dorsal skin bold area during the experiment  $\pm$  SEM is represented; \* $P < 0.01$ , \*\* $P < 0.005$ .

To further refine this striking observation, we performed a series of large-scale analysis of gene expression using mRNA microarrays and back skin target samples obtained at 50 and 90 days after birth in basal conditions. Interestingly, we found that the large-scale gene expression signature was essentially equivalent in *Eng*<sup>+/+</sup> and *Eng*<sup>+/-</sup> littermates at the entry of the refractory telogen (postnatal day 50) but differed significantly in the competent telogen/anagen transition (postnatal day 90), when hair follicle stem cell niches are able to respond to stimulatory signals (Plikus et al., 2008) (Supplementary Figure S6A). At postnatal day 90, several genes, belonging to different gene ontology groups, were found differentially up- or downregulated in either *Eng*<sup>+/+</sup> or *Eng*<sup>+/-</sup> animals, many of them related to the regulation of hair follicle growth (Supplementary Figure S6B and C). These results are in close agreement with the *Eng* expression profile during the hair follicle cycle, showing a low expression level at the entry into refractory telogen (postnatal day 50) and a high expression in the competent telogen/anagen transition (postnatal day 90). In addition, these results fit well with the observation that *Eng*<sup>+/+</sup> and *Eng*<sup>+/-</sup> resting hair follicles contain a similar number of resident stem cells that deficiently respond to a proliferative stimulus in *Eng* haploinsufficiency conditions. These observations suggest that a right *Eng* expression level is required at specific time points of the hair follicle to establish an adequate gene expression pattern.

*Eng haploinsufficiency is associated with a defective proliferative response to growth stimulation of hair follicle bulge stem cells*

Taking into account that the hair follicle growth cycle is ultimately regulated by the activity of skin stem cells, we next investigated the effect of a functional reduction of *Eng* in the proliferative potential of the bulge skin stem cell population. To this end, we first proceeded to identify bulge stem cells as label retaining cells (LRCs) in pulse and long-chase experiments with the nucleotide analogue 5-bromo-2'-deoxyuridine (BrdU) (Braun et al., 2003). We quantified the number of LRCs in the bulge region of hair follicles at 55 days after birth, during which time hair follicles are in the telogen or resting phase and are insensitive to stimulatory signals (Mu et al., 2001). Under these resting conditions, the number and location of LRCs in the bulge region of hair follicles were essentially equivalent in *Eng*<sup>+/+</sup> and *Eng*<sup>+/-</sup> littermates (Figure 4A). Next, we used the phorbol ester TPA to stimulate cell proliferation in the skin and in the hair follicle (Cotsarelis et al., 1990; Braun et al., 2003; Espada et al., 2008). Upon stimulation, wild-type animals showed a significant increase of LRCs in the bulge region, as expected (Figure 4A). However, *Eng*<sup>+/-</sup> animals significantly failed to trigger LRC proliferation in the hair follicle (Figure 4A). These results were corroborated by using a different procedure to activate bulge stem cell proliferation, namely the induction of a transient reactive oxygen species (ROS) production in the skin (Carrasco et al., 2015) (Supplementary Figure S7), suggesting that *Eng* haploinsufficiency directly affects the proliferative response of skin stem cells to growth signals.

To further confirm the loss of proliferative potential in the skin and, particularly, in the bulge region of the hair follicle in *Eng*<sup>+/-</sup> mice, we quantified the number of proliferating cells after a short BrdU pulse in adult animals before and after TPA stimulation in different regions of telogen hair follicles and in the interfollicular epidermis (IFE). We found that in the absence of a proliferative stimulus, the number and location of proliferating cells were similar in *Eng*<sup>+/+</sup> and *Eng*<sup>+/-</sup> mouse epidermis (Figure 4B). However, after TPA stimulation, a significantly reduced number of proliferating cells in the bulge region, the infundibulum, and the IFE was quantified in *Eng*<sup>+/-</sup> mice, compared with control *Eng*<sup>+/+</sup> littermates (Figure 4B). We also performed TUNEL assays to rule out the possibility of cell death induction as cause for the loss of proliferative potential in the skin of *Eng*<sup>+/-</sup> mice (Supplementary Figure S8). In addition, we quantified by qRT-PCR the expression of two defined stem cell markers, Ck15 and Cd34 in back skin in response to TPA treatment. The results obtained in back skin at Days 50 and 90 (Supplementary Figure S9) strongly corroborate and support the results obtained in tail skin, indicating that the ability of the hair follicle stem cell niche to respond to a proliferative stimulus is impaired in *Eng*<sup>+/-</sup> animals. As a whole, these results indicate that *Eng* haploinsufficiency does not alter the number of resident hair follicle bulge stem cells in a resting (telogen) phase but is associated to a defective proliferative response after cell growth stimulation, e.g. after the induction of anagen entry.

*Eng haploinsufficiency reveals a cross-talk mechanism between Wnt/ $\beta$ -catenin and Bmp/Smad signalling pathways during the hair follicle cycle*

In our biological model, *Eng* gene expression is activated about postnatal day 50 (autonomous anagen/refractory telogen transition) (Figure 1A and Supplementary Figure S1) after Wnt/ $\beta$ -catenin signalling was operational and Bmp/Smad signalling has been recently activated to slow down hair growth (Plikus et al., 2008). From this point, *Eng* expression steadily increases throughout the telogen phase and drastically decreases at the competent telogen/propagant anagen transition. After that point, in propagant anagen, Wnt/ $\beta$ -catenin signalling is reactivated (Plikus et al., 2008), while Bmp/Smad signalling is completely switched off (Figure 1A and Supplementary Figure S1). Thus, the *Eng* promoter is transcriptionally active when both Wnt/ $\beta$ -catenin and Bmp/Smad signals are switched on; this transcriptional activity is maintained when Wnt/ $\beta$ -catenin signal is switched off, continues being strongly repressed when Bmp/Smad signalling is switched off, and increases again its expression when Wnt/ $\beta$ -catenin signalling is reactivated (Figure 1A).

In this context, we hypothesized that an *Eng*-dependent cross-talk mechanism between Wnt/ $\beta$ -catenin and Bmp/Smad signalling may act at this point of the hair follicle cycle, a function predicted for feedback target regulators in the dual oscillator model of hair follicle dynamics (Plikus et al., 2011; Tasseff et al., 2014; Baik et al., 2016). We first wondered if  $\beta$ -catenin could interact with the *Eng* promoter as part of a molecular toggle to interconnect both signalling pathways. Indeed, we found that  $\beta$ -catenin strongly

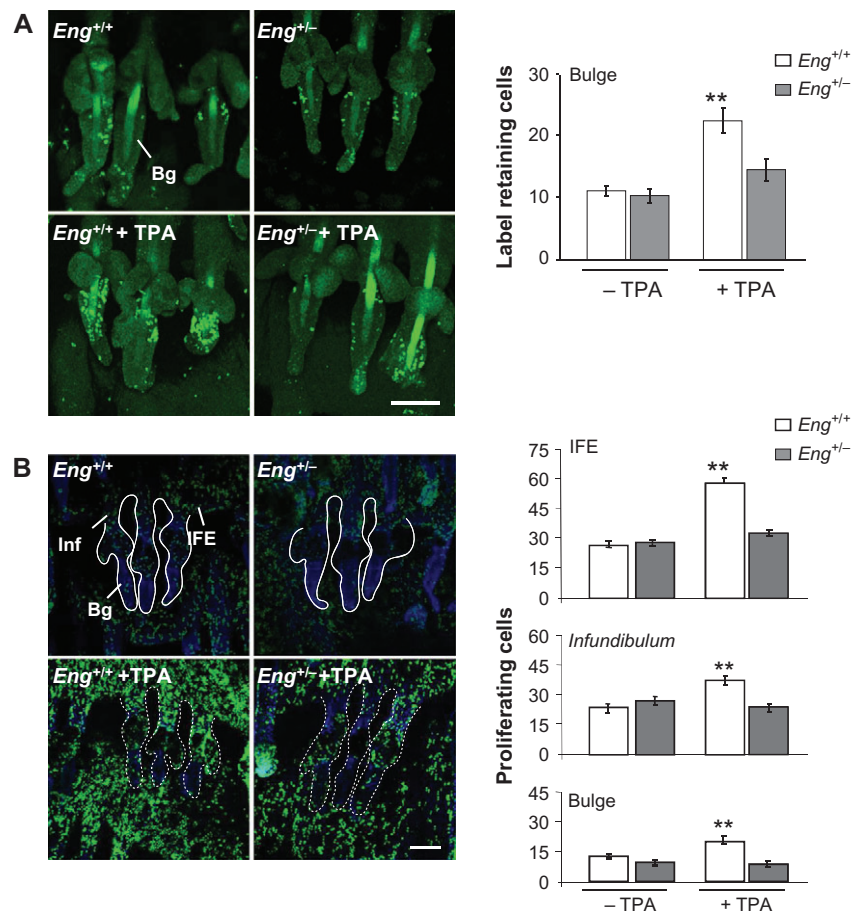


**Figure 4** Endoglin haploinsufficiency is associated with a defective proliferative response in the mouse skin and hair follicle bulge stem cell niche after cell growth stimulation. **(A)** Quiescent bulge (Bg) stem cells in resting tail hair follicles (telogen, postnatal day 50) were identified as BrdU LRCs after a long chase period following neonatal labelling (left panels) and quantified (right panels; the mean  $\pm$  SEM is represented,  $n = 3$ ;  $**P < 0.005$ ). Under basal conditions, *Eng*<sup>+/+</sup> and *Eng*<sup>+/-</sup> mice showed a similar number of LRCs in the bulge region. However, the proliferative response of these cells after cell growth stimulation with the phorbol ester TPA, identified as a significant increase in the number of LRCs, was severely impaired in *Eng*<sup>+/-</sup> mice. **(B)** Proliferating cells in resting tail skin and hair follicles were identified as positive BrdU cells after a short labelling pulse in adult animals (left panels) and quantified (right panels; the mean  $\pm$  SEM is represented,  $n = 3$ ;  $**P < 0.005$ ). A widespread defective proliferative response after cell growth stimulation with TPA was observed in *Eng*<sup>+/-</sup> animals in most skin locations, including the IFE, the infundibulum (Inf), and the bulge region (Bg). In all cases, representative confocal microscopy images (maximum projections) corresponding to whole-mounts of tail skin epidermis are shown. Scale bar, 100  $\mu$ m.

binds the *Eng* promoter transcription start site (-52/+132) in the skin of *Eng*<sup>+/+</sup> mice during autonomous anagen/refractory telogen transition (postnatal day 50), but not during the competent telogen/propagant anagen transition (postnatal day 90) (Figure 5A). As expected, this binding was not observed in *Eng*<sup>+/-</sup> littermates (Figure 5A). These observations are in close agreement with the pattern of *Eng* expression during the hair follicle and suggest that Bmp/Smad signalling is required for the binding of  $\beta$ -catenin to the *Eng* promoter. This is confirmed by the fact that in *Eng*<sup>+/-</sup> animals, a reduction of functional Eng (Figure 1A) impairs Bmp signalling (Figure 2A), despite expressing similar levels of Bmp during the hair cycle to their *Eng*<sup>+/+</sup> littermates, and this coincides with the absence of the interaction of  $\beta$ -catenin to the *Eng* promoter (Figure 5A).

To corroborate the feasibility of this molecular mechanism in a tissue independent context, we used the mouse embryonic E14 cell line. This cell line shows a constitutive accumulation of cytoplasmic  $\beta$ -catenin, driven by LIF-containing media (Takao et al., 2007), mimicking the steady levels of this protein that are observed during the hair follicle cycle in mouse back skin. In this molecular background, we treated E14 cultures with Bmp4 to mimic the anagen/refractory telogen transition and the *Eng* mRNA was depleted by using siRNA interference to mimic *Eng* haploinsufficiency (Figure 5B and Supplementary Figure S10). We found that this model system suitably recapitulated the binding pattern of  $\beta$ -catenin to the *Eng* promoter observed in mouse skin, requiring Bmp4 and *Eng* expression to occur (Figure 5B).

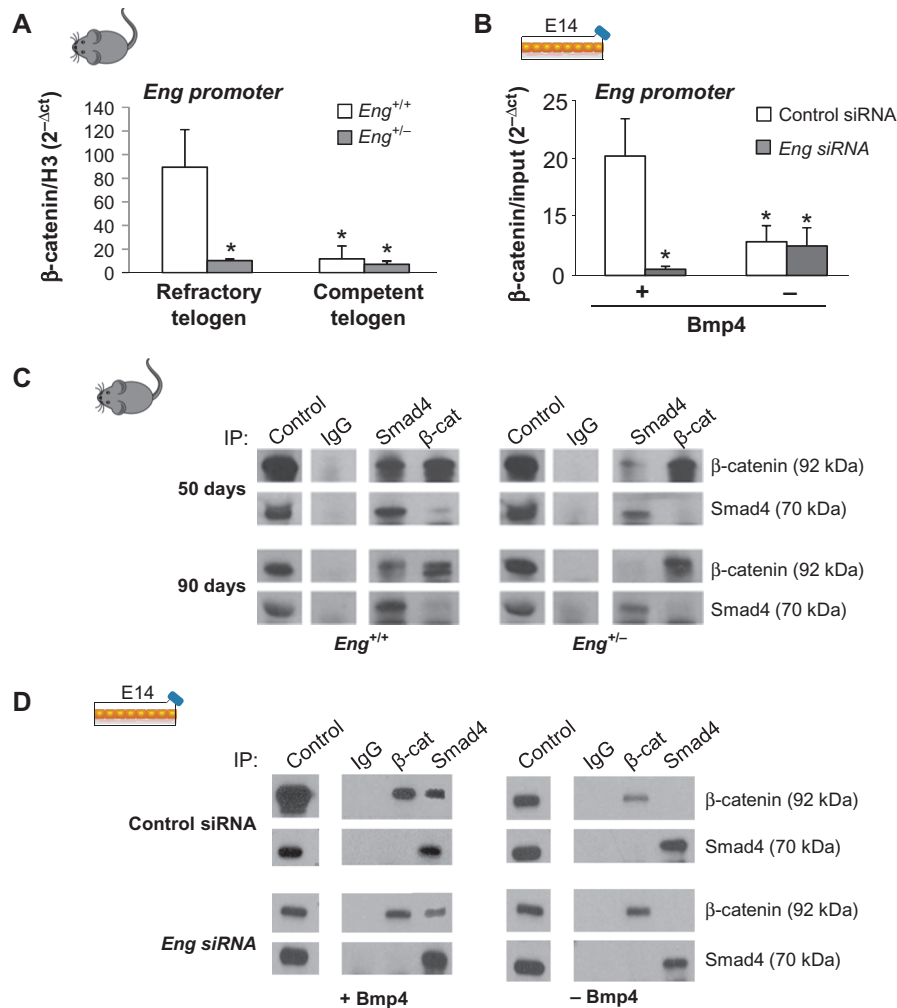


**Figure 5**  $\beta$ -catenin directly binds to the *Eng* promoter and interacts with Smad4 depending on Bmp4 signalling and *Eng* expression. (**A** and **B**) Analysis of the interaction of  $\beta$ -catenin with the *Eng* promoter transcriptional start site ( $-52/+132$  bp) by quantitative ChIP in *Eng*<sup>+/+</sup> and *Eng*<sup>+/-</sup> mouse samples of dorsal skin during the anagen/refractory telogen transition (postnatal day 50) or the competent telogen phase (postnatal day 90) (**A**) and E14 mES cells transiently transfected with *Eng* siRNA or control siRNA and treated with Bmp4 or vehicle control to mimic *Eng*<sup>+/-</sup> and *Eng*<sup>+/+</sup> tissue microenvironment during refractory or competent telogen, respectively (**B**). ChIP assays were normalized to histone H3 (**A**) or input signals (**B**). Results shown are representative of three experiments in triplicate samples. The mean  $\pm$  SE is represented;  $*P < 0.01$ . (**C** and **D**) Analysis of the interaction between  $\beta$ -catenin and Smad4 proteins by co-immunoprecipitation analysis in *Eng*<sup>+/+</sup> and *Eng*<sup>+/-</sup> mouse samples of dorsal skin during the anagen/refractory telogen transition (postnatal day 50) or the competent telogen phase (postnatal day 90) (**C**) and E14 cell cultures transiently transfected with *Eng* siRNA or control siRNA and treated with Bmp4 or vehicle control to mimic *Eng*<sup>+/-</sup> and *Eng*<sup>+/+</sup> tissue microenvironment during refractory or competent telogen, respectively (**D**). Results shown are representative of three experiments, using pools of triplicate samples in each lane.

The requirement of Bmp4 for the binding of  $\beta$ -catenin to the *Eng* promoter suggests that Smad4, the common transducer of Bmp signalling that is translocated to the nuclear compartment to activate specific gene expression (Heldin et al., 1997; Lebrin et al., 2004; Blitz and Cho, 2009), could be involved in this mechanism. We reasoned that an interaction between  $\beta$ -catenin and Smad4 could drive *Eng* promoter activation. To test this hypothesis, we first performed a series of co-immunoprecipitation experiments in skin samples obtained in the anagen/refractory telogen transition (postnatal day 50) or in the competent telogen/propagant anagen transition (postnatal day 90). The results

obtained indicated that in *Eng*<sup>+/+</sup> mice,  $\beta$ -catenin strongly interacts with Smad4 at the onset of the refractory telogen, coinciding with the co-expression of both proteins in the tissue (Figure 5C). This specific interaction was lost in *Eng*<sup>+/-</sup> littermates (Figure 5C), mirroring the loss of  $\beta$ -catenin binding to the *Eng* promoter. The interaction between  $\beta$ -catenin and Smad4 was also significantly diminished at Day 90, during the competent telogen in both *Eng*<sup>+/+</sup> and *Eng*<sup>+/-</sup> littermates (Figure 5C), when Bmp/Smad and Wnt/ $\beta$ -catenin pathways are not activated (Figure 2A and Supplementary Figure S1). In addition, this pattern of  $\beta$ -catenin/Smad4 interactions in mouse skin was recapitulated in the E14 cell model (Figure 5D).



It is to note that in both mouse skin and E14 cells, the interaction of  $\beta$ -catenin/Smad4 in co-immunoprecipitation assays was easily observed using an anti-Smad4 antibody but to a lesser extent using an anti- $\beta$ -catenin antibody. This is an interesting observation since this anti- $\beta$ -catenin antibody has been previously used in numerous studies to report the binding of  $\beta$ -catenin with different partners (Espada et al., 1999, 2005). We further used the E14 cell model to demonstrate that Smad4 is required for the  $\beta$ -catenin binding to the *Eng* promoter induced by Bmp4 (Supplementary Figure S11). As a whole, these results suggest that *Eng* is essential for both  $\beta$ -catenin promoter binding and  $\beta$ -catenin/Smad4 interaction processes, probably due to its key role as a component of the Bmp receptor complex.

In this context, we finally tested the potential of  $\beta$ -catenin, Smad4, or a combination of both proteins to regulate the transcriptional activity of the *Eng* promoter. To this end, we performed a series of promoter activation assays in human embryonic kidney 293T cells. This cell line does not express significant levels of endogenous  $\beta$ -catenin, Smad4, or *Eng* (Figure 6A), providing a suitable model to analyse the effect of these proteins on the activity of the *Eng* promoter. In this cellular background, expression of activated  $\beta$ -catenin increases *Eng* protein levels and this effect is synergistically potentiated by co-

expression of Smad4 (Figure 6A). Moreover, we found that activated  $\beta$ -catenin efficiently activates a reporter plasmid containing the -2450/+350 bp promoter region of the *Eng* gene and this activation was strongly increased when both activated  $\beta$ -catenin and Smad4 were co-expressed (Figure 6B). Interestingly, a high *Eng* expression is observed in the mouse back skin when high levels of  $\beta$ -catenin and Smad4 are present in the tissue (refractory telogen, postnatal day 70), but a significant reduction of *Eng* expression is observed when Smad4 levels decay (propagant anagen, postnatal day 100) (Figure 6C). These results indicate that the  $\beta$ -catenin/Smad4 heterodimer is an efficient activator of the *Eng* promoter transcriptional activity.

## Discussion

Here we provide evidence of an important role for the Tgf- $\beta$ /Bmp co-receptor *Eng* in the molecular switch between Wnt/ $\beta$ -catenin and Bmp/Smad signalling that occurs during the hair follicle growth cycle. We have found that *Eng* shows a highly defined expression pattern in the skin related to the hair growth cycle phase and to the proliferative state of the resident skin stem cell population, suggesting that *Eng* levels are an important factor on the whole homeostatic regulation of this tissue. These observations are in agreement with other reports demonstrating that *Eng* expression can oscillate

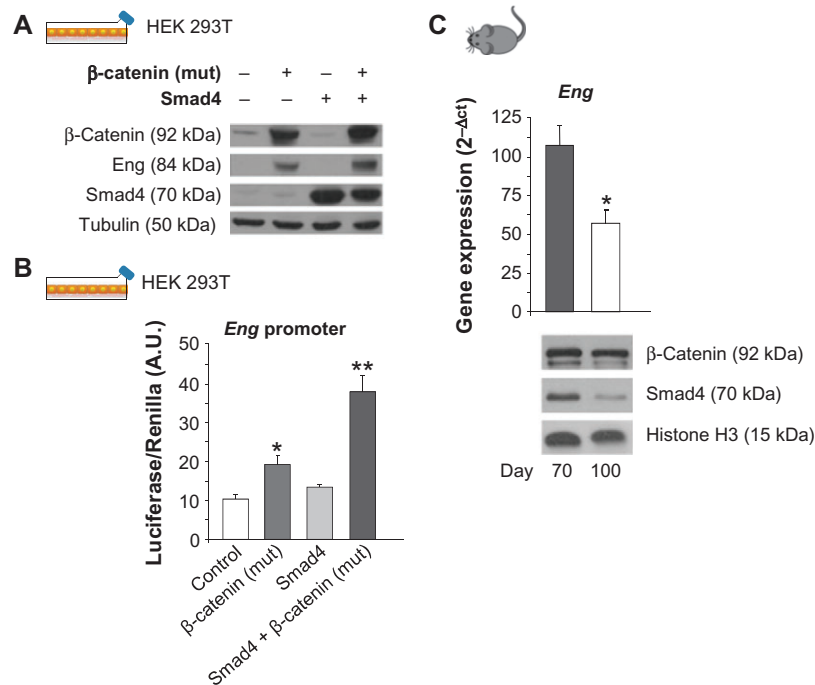


**Figure 6**  $\beta$ -catenin and Smad4 synergistically promote the transcriptional activation of the *Eng* promoter and subsequent *Eng* protein expression. (A) Immunoblot analysis of  $\beta$ -catenin, Smad4, and *Eng* protein expression levels in 293T cells after transient transfection with  $\beta$ -catenin and Smad4 expression vectors. Tubulin expression was used as loading control. Results are representative of three experiments, using triplicate samples. (B) Luciferase reporter assays of *Eng* promoter activity in 293T cells after transient transfection of  $\beta$ -catenin and Smad4 expression vectors. The mean  $\pm$  SE of luciferase/Renilla normalized signals (A.U., arbitrary units) of three independent experiments is represented. (C) *Eng* mRNA expression quantification by qRT-PCR, normalized to 18S rRNA, in wild-type mouse dorsal skin during the refractory telogen (postnatal day 70) or the propagant anagen (postnatal day 100) of the hair growth cycle (upper panel; the mean  $\pm$  SEM is represented,  $n = 3$ ;  $*P < 0.01$ ) and immunoblot analysis of  $\beta$ -catenin and Smad4 at the same time points, using histone H3 as loading control (lower panels; results are representative of triplicate samples).

in the endothelium to act as a modulatory switch between angiogenesis and quiescence programs in the tissue, promoting either Tgf- $\beta$ /Alk5 or Tgf- $\beta$ /Alk1 signalling, respectively (Paus et al., 1999; Botella et al., 2001; López-Novoa and Bernabeu, 2010). Mutations in *Eng* causing the autosomal dominant bleeding disorder hereditary haemorrhagic telangiectasia type I (HHT1) are associated to a severe alteration of this signalling balance (McAllister et al., 1994; Lebrin et al., 2004; Sanz-Rodríguez et al., 2004; López-Novoa and Bernabeu, 2010; Kapur et al., 2013). The reduced proliferative potential of bulge LRCs after a growth stimulus is also in close consonance with the finding that reduced *Eng* expression is associated to a delayed wound healing in the skin (Pérez-Gómez et al., 2014).

Both the hair follicle cycle-dependent expression pattern of *Eng* in the skin and its involvement in the hair follicle proliferative stem cell response identify *Eng* as a potential feedback regulator target predicted in a coupled dual oscillator model of the hair follicle growth cycle (Tasseff et al., 2014). In this model, cyclic hair follicle dynamics is precisely described and recapitulated as the result of two interacting cell populations, mesenchymal (niche cells) and epithelial (stem cells), showing an out-of-phase synchronized pattern of gene expression. The growth of the hair follicle is mainly driven by the epithelial cell population and this activity is regulated in a feedback pattern by the background mesenchymal cell population through direct cross-talk mechanisms. In this model, it is predicted that the feedback cross-talk between both populations will be mainly regulated by key targets, which is further identified according to the previously published data of whole-gene expression patterns in mouse skin. Using this novel approach, *Eng* was identified as one of these key targets, and the results that we report in this work fully support the role for this protein in the skin predicted by the coupled dual oscillator model.

In this sense, we have accordingly found that a reduced level of *Eng* expression in the skin is associated with the deregulation of the hair follicle cycle, resulting in a delayed establishment of refractory telogen phase. Moreover, we have shown that stimulation of hair growth during the refractory or competent telogen phases of the hair follicle has strikingly different outputs depending on the *Eng* expression background. Interestingly, alterations in the hair cycle associated to mutations in cytokines and receptors involved in Tgf- $\beta$ /Bmp signalling have been previously reported. Thus *Tgf- $\beta$ 2* mutations result in a delayed anagen establishment (Oshimori and Fuchs, 2012) while *Tgf- $\beta$ 1*<sup>-/-</sup> mice show a delayed catagen establishment during the first postnatal cycle (Foitzik et al., 2000; Lin and Yang, 2012). Also, overexpression of the Bmp antagonist Noggin in the mouse epidermal basal layer results in a dramatically shortened refractory telogen phase and an accelerated propagation of the hair follicle regenerative wave (Plikus et al., 2008; Lin and Yang, 2012), while subcutaneous Bmp4 injections inhibit anagen establishment (Plikus et al., 2008). These observations point to an essential role for Tgf- $\beta$ /Bmp in the feedback mechanisms that regulate the inhibition of hair growth, and suggest that *Eng*, as a part of the Tgf- $\beta$ /Bmp receptor complex (Cheifetz et al., 1992; Shi and Massagué, 2003), which in turn controls the

establishment of the refractory telogen (Plikus et al., 2008), is a central element in the regulation of hair follicle dynamics.

Bmp/Smad 1/5/8 and Tgf- $\beta$ /Smad 2/3 have different signalling roles, even antagonistic, during the mouse hair follicle. It has been reported that impairment of BMP signalling by conditional deletion of the receptor Bmpr1a stimulates the proliferation of quiescent hair follicle stem cells, while sustained BMP signalling promotes a premature hair follicle differentiation (Kobielak et al., 2007). However, Bmp signalling is also required by dermal papilla cells to induce hair follicle growth (Rendl et al., 2008) and regulates the progression of the hair follicle stem cell-derived transit amplifying lineages through Smad 1/5/8 target genes (Genander et al., 2014). On the other hand, Tgf- $\beta$  signalling has been directly implicated in the induction and progression of the regression (catagen phase) of the hair follicle cycle (Foitzik et al., 2000; Lin and Yang, 2013). It has been also reported that disruption of Tgf- $\beta$  signalling results in defective proliferation and maintenance of bulge hair follicle stem cells (Lin and Yang, 2012). Moreover, Tgf- $\beta$  signalling can antagonize the BMP-mediated repression of hair follicle stem cell activation (Oshimori and Fuchs, 2012). All of these results manifest the complex interplay of the Bmp/Tgf- $\beta$ /Smad signalling network in the regulation of the hair follicle cycle and associated stem cell niches. In this context, the results reported here indicate that *Eng* may play a role in the dynamic choice between Bmp or Tgf- $\beta$  signalling during different phases hair follicle cycle. The impaired response of bulge stem cells to proliferative stimuli suggests that *Eng* can modulate Tgf- $\beta$ /Smad signalling during the activation of hair follicle stem cell niches. This important aspect deserves further investigation.

Different reports point to a cross-talk between Wnt/ $\beta$ -catenin and Tgf- $\beta$ /Bmp signalling as a basic regulatory mechanism of stem cell function in mammalian tissues; for instance, in the regulation of intestine stem cells proliferation (He et al., 2004; Kühl and Kühl, 2013), epidermal/hair placode fate (Fuchs, 2007), or, more recently, in haematopoiesis, where *Eng* integrates Bmp and Wnt signalling to induce that process (Baik et al., 2016). However, the underlying molecular mechanisms are not well characterized particularly in the hair follicle cycle. Here we have used the theoretical framework of the coupled dual oscillator model of hair follicle dynamics (Tasseff et al., 2014) to identify *Eng* as a potential key regulator of the feedback cross-talk between these signalling pathways. Supporting this notion, we have found that, in mouse skin, *Eng* expression increases after anagen establishment, a time point in which  $\beta$ -catenin becomes transcriptionally competent due to Wnt signalling activation (Fuchs, 2007; Kühl and Kühl, 2013). Moreover, our results show that during the mouse hair follicle cycle  $\beta$ -catenin directly interacts with the transcription start site of *Eng* promoter in an *Eng*/Bmp4-dependent manner, and this binding is associated to *Eng* transcription. These results are fully recapitulated in the E14 embryonic cell model, suggesting that this is a universal mechanism. In addition, we have also found that in both mouse skin and E14 cells,  $\beta$ -catenin interacts with the Bmp signal transducer Smad4 in an *Eng*/Bmp4-dependent manner,

and that both proteins can act synergistically to activate the *Eng* promoter. Also, the  $\beta$ -catenin–*Eng* promoter interaction is completely abolished when the expression of *Smad4* mRNA is inhibited. These observations are in agreement with the fact that *Eng* expression can be regulated in a feedback pattern by the signalling pathways in which it is involved (Botella et al., 2001; Baik et al., 2016).

As a whole, the results reported here indicate that *Eng* is a key component of the molecular oscillator that regulates the hair follicle cycle, acting as an important element in the dynamic cross-talk between Wnt/ $\beta$ -catenin and Tgf- $\beta$ /Bmp signalling. This cross-talk would consist in a feedback mechanism in which *Eng* expression is regulated by  $\beta$ -catenin binding to the *Eng* promoter in a pattern dependent on Bmp4 signalling and further driven by the interaction of  $\beta$ -catenin with the Bmp4 transducer Smad4, and in turn, as recently demonstrated, *Eng* induction enhances Wnt activity that promotes the stabilization of activated Smads (Baik et al., 2016), establishing a negative feedback that points *Eng* as a potential universal oscillator. As *Eng* is required to transmit the Bmp4 signal and to mobilize Smad4, a  $\beta$ -catenin-dependent transcriptional activation of *Eng* expression suitably close the feedback circuit. It is tempting to speculate that a similar or equivalent mechanism could be found in mammalian tissues in which a coordinated Wnt/ $\beta$ -catenin and Tgf- $\beta$ /Bmp/Smad signalling cross-talk is involved in the regulation of tissue homeostasis, bringing to the forefront a new research framework to investigate adult stem cell biology.

## Material and methods

### Cell culture procedures

The feeder-independent E14 mouse embryonic stem (ES) and human embryonic kidney 293T cell lines were used in this study. E14 cells (a gift from T. Rodriguez, Imperial College, London) were grown on 0.1% gelatin-coated flasks in GMEM supplemented with 10% FCS, NEAA, L-glutamine, pyruvate,  $\beta$ -mercaptoethanol (all from Gibco), and 1000 U/ml LIF (Millipore), and splitted 1:8 or 1:10 every 2–3 days using Trypsin-EDTA (Invitrogen) (Smith, 1991; Cambray et al., 2012). 293T cells were cultured in DMEM supplemented with 10% FCS, L-glutamine and antibiotics, and divided 1:10 or 1:20 every 2–3 days using trypsin-EDTA (Invitrogen). Both cell lines were maintained at 37°C in a 5% CO<sub>2</sub> humidified atmosphere.

For Bmp pathway activation, E14 cell cultures were serum starved from 4 to 12 h and subsequently treated for 1.5 h with 10 ng/ml of recombinant mouse Bmp4 protein (R&D Systems), or BSA at the same concentration as vehicle control.

For *Eng* RNA interference in E14 cells, a siRNA cocktail containing 4 different oligonucleotides (50 nM each) targeting different regions of the coding sequence was used (Qiagen, S1009938-11, –18, –25, –32). For Smad4 RNA interference in E14 cells, an esiRNA was used, consisting of a endoribonuclease-prepared siRNA pool comprised of a heterogeneous mixture of siRNAs that all target the Smad4 mRNA sequence (Sigma Aldrich Smad4 Mission® esiRNA1, 25 nM). MISSION® siRNA Universal Negative Control #1 was used as negative control for siRNA transfection

(Sigma-Aldrich, 25 nM). Transcriptional inhibition of gene targets was evaluated by qRT-PCR.

For protein overexpression experiments, pcDNA3-Smad4 (Kang et al., 2005) and pCI-neo-mutant  $\beta$ -catenin (S33Y) (Morin et al., 1997; Espada et al., 2005) constructs were transiently transfected in 293T cells. Protein expression levels were evaluated by immunoblotting. For *Eng* promoter expression assays, pCD105 (–50/+350) and pCD105 (–2450/+350) reporter constructs derived from the human *ENG* promoter were used as described (Botella et al., 2002). Luciferase reporter activity was determined in whole cell lysates using the dual GLO-luciferase assay kit (Promega) and Renilla expression vector as an internal control, following the manufacturer's instructions. The empty luciferase vector pXP2 was used as control. The amount of DNA in each transfection was normalized using the corresponding empty vector. In all cases, transfection assays were performed using Lipofectamine® 2000 transfection reagent (Life Technologies) following manufacturers' instructions.

### Animal procedures

Generation, maintenance, and genotyping of an *Eng*<sup>+/–</sup> mouse strain on a C57Bl/6 background have been previously described (Bourdeau et al., 1999). Animals were kept in ventilated rooms under lighting (12-h light, 12-h dark cycle) and temperature-controlled conditions and allowed feed and water *ad libitum*. All experiments were conducted in parallel in *Eng*<sup>+/–</sup> and *Eng*<sup>+/+</sup> littermate mice aged 1–5 months. All experimental procedures were conducted in compliance with 2010/63/UE European guidelines.

Induction of hair growth was basically performed at two different points during the hair follicle cycle: anagen/refractory telogen transition (postnatal day 50) and competent telogen/anagen transition (postnatal day 90) (Plikus and Chuong, 2008; Plikus et al., 2009). Haired back skin regions of at least 3 mice of each genotype and each hair cycle phase were clipped as described (Carrasco et al., 2015). Progression of hair growth was sequentially monitored and imaged daily until most animals of one genotype completed fully hair coating. Hair clipping was chosen over plucking or shaving to avoid wounding that can potentially interfere with normal hair growth (Chase, 1954; Plikus and Chuong, 2008).

Activation of skin stem cell and transit amplifying cell proliferation and mobilization in back and tail skin was performed by sequential (3 times) topical application of three doses of 20 nM 12-O-Tetradecanoylphorbol-13-acetate (TPA, Sigma-Aldrich) (Fürstenberger and Marks, 1980; Braun et al., 2003; Espada et al., 2008). Skin stem cell proliferation was also activated by induction of a transient production of ROS in the tissue as previously described (Fischer et al., 1986; Carrasco et al., 2015).

### Immunological procedures

Antibodies used in this work are listed in Supplementary Table S1.

For immunolocalization of proteins in histological sections, pieces of dorsal skin were fixed in pH 7.0 buffered 3.7% formaldehyde and processed for histology. Histological sections were

stained with the indicated antibodies after permeabilization in 0.1% Triton X-100, except in the case of *Eng* detection, and blocked in 0.5% BSA. The immunofluorescent signal was revealed using HRP-coupled secondary antibodies and TSA Plus Cyanine 3 (Perkin Elmer) for signal amplification, following the manufacturer's instructions. Histological sections were also stained with standard haematoxylin-eosin for routine evaluation of tissue morphology.

For the preparation of tail epidermis whole-mounts, tails were clipped, and the skin was peeled and treated with 5 mM EDTA. Intact sheets of epidermis were separated from the dermis and fixed in pH 7.0 buffered 3.7% formaldehyde. For BrdU detection in whole-mounts, intact sheets of epidermis were washed in PBS several times in order to remove excess of formaldehyde, and treated with HCl (5 N) for nuclear acid hydrolysis, followed by TBE (Tris-Borate-EDTA) for neutralization. After blocking and permeabilization with PBT buffer (0.5% Triton X-100 and 0.2% gelatine in PBS), epidermis sheets were stained with FITC-conjugated mouse monoclonal anti-BrdU, as previously described (Braun et al., 2003). For apoptosis detection in hair follicles of tail epidermis, TUNEL Label (Roche) assay was performed.

Confocal images were obtained in Leica TCS SP2 and SP5 AOBS spectral confocal microscope and processed using the Fiji software (Image J 1.49, National Institutes of Health).

For immunoblotting, cell pellets or whole skin samples were homogenized in RIPA (25 mM Tris-HCl pH 7.6, 150 mM NaCl, 1% NP-40, 0.1% SDS) or SDS buffer (50 mM Tris-HCl pH 6.8, 2% SDS, 10% glycerol, 1%  $\beta$ -mercaptoethanol, 12.5 mM EDTA) containing protease and phosphatase inhibitors (2  $\mu$ g/ml aprotinin, 2 mM PMSF, 2  $\mu$ g/ml leupeptin and 2 mM sodium orthovanadate, 2 mM  $\beta$ -glycerophosphate, 5 mM NaF, all from Sigma-Aldrich). Skin samples were fully disaggregated using scissors and a Polytron® homogenizer (PT 1200 E, Kinematica), and the same amount of protein of each mouse was loaded in Laemmli buffer. Proteins were resolved in a 7.5% SDS-PAGE system and were transferred to a PVDF membrane, which was blocked and stained with the indicated primary and secondary HRP conjugated antibodies. Finally, HRP activity was detected using the ECL-chemiluminescent kit (Amersham) in accordance with the manufacturer's instructions.

For Chromatin Immunoprecipitation (ChIP) assays the ENCODE and modENCODE guideline standards for ChIP experiments and data analysis (ENCODE Consortium V 2.0, 2011) were followed. Cell pellets and skin samples disaggregated with scissors were fixed in 1% formaldehyde-PBS, disaggregated and processed in ChIP lysis buffer (1% SDS, 10 mM EDTA, 50 mM Tris-HCl, pH 8.0) with protease and phosphatase inhibitors (2  $\mu$ g/ml aprotinin, 2 mM PMSF, 2  $\mu$ g/ml leupeptin and 2 mM sodium orthovanadate, 2 mM  $\beta$ -glycerophosphate, 5 mM NaF, all from Sigma-Aldrich). Supernatants were sonicated and cellular debris was removed by centrifugation. To evaluate proteins binding to the *Eng* promoter, supernatants were incubated with the indicated primary antibodies, DNA-protein interaction was reversed, and qRT-PCR or conventional PCR were performed using the DNA *mEng* primers Fwd3 and Rvs3 (Supplementary Table S2).

For protein co-immunoprecipitation assays, cell pellets or skin samples were homogenized in IPH buffer (50 mM Tris-HCl pH 7.4, 100 mM NaCl, 10% glycerol, 5 mM EDTA, 0.15% Triton X-100) containing protease and phosphatase inhibitors as described before. Skin samples were disaggregated using scissors, and the supernatant was incubated O/N with the indicated antibodies and the equivalent IgG as a negative control. Proteins were resolved in a 7.5% SDS-PAGE system and transferred to PVDF membranes that were incubated with the indicated primary and secondary antibodies.

#### Gene expression procedures

For RNA extraction, E14 cell cultures coming from the treatments described above, or whole dorsal skin of at least three mice at each time point and genotype, RNeasy mini kit and RNase-Free DNase Set (both from Qiagen) were used. Skin tissue was homogenized using TriPure™ isolation Reagent (Roche), disaggregated and processed using scissors and a Polytron® homogenizer (PT 1200 E, Kinematica). For reverse transcription, MLV enzyme (Promega) was used, loading the same amount of RNA. qRT-PCR or semiquantitative PCR assays were performed for gene expression analysis, using Power SYBR Green (Applied Biosystems) or REExtract-N-Amp™ PCR ReadyMix™ (Sigma Aldrich), respectively, following manufacturer's instructions. Specific primers, detailed in Supplementary Table S2, were designed among different exons, thereby avoiding residual genomic DNA amplification, for semiquantitative or quantitative transcript detection.

Microarray experiments were performed using Mouse Gene Expression 4x44K Microarray Kit G4122F (Agilent Technologies). RNA was isolated using RNAeasy Extraction Kit (QIAGEN). RNA was labelled and array hybridized using the Low RNA Linear Amplification Kit and the In Situ Hybridization Kit Plus (Agilent Technologies) respectively. After hybridization and washing, the slides were scanned in an Axon GenePix Scanner (Axon Instruments Inc.) and analysed using Feature Extraction Software 10.1 (Agilent Technologies). Two different RNA samples obtained from each *Eng* modified cell line were labelled with Cy5-dUTP. The RNA samples extracted from wild-type cells were marked with Cy3-dUTP (Amersham). Two additional hybridizations were performed using the reciprocal fluorochrome labelling. The genes whose expression was up or downregulated at least 2-fold in *Eng*<sup>+/-</sup> with respect to control cells were selected for analysis. Microarray raw data have been deposited in the Gene Expression Omnibus under the accession number of GSE120556 (submitter G. M.-B.).

#### Statistical analysis

Quantifications of LRC in the bulge region were performed on confocal images (30 hair follicles/animal, 3 animals/group). Comparisons between groups were performed by Student's *t*-test using the SPSS 15.0 software (IBM). For statistical analyses of gene expression data, an unpaired *t*-test was applied, setting  $P \leq 0.05$  as limit for significance. Quantitative real-time reverse-transcriptase-PCR data were analysed using a comparative CT method, by using 18S ribosomal RNA expression as an internal control. Gene expression changes were represented as



$2^{-\Delta Ct}$  values of the mean values of *Eng*<sup>+/-</sup> and control groups at different time points during the second postnatal hair growth cycle. For quantification of hair regeneration, day-to-day digital images were analysed. The bold area was quantified using the Fiji software. The area under the curve was calculated separately for each mouse, and means were compared by the Student's *t*-test. For statistical analysis of luciferase reporter activity between the experimental samples, an unpaired *t*-test was applied setting *P* ≤ 0.05 as limit for significance. Transactivation assay results were expressed as the ratio between luciferase activity and Renilla expression vector as an internal control.

### Supplementary material

Supplementary material is available at *Journal of Molecular Cell Biology* online.

### Acknowledgements

We thank Michelle Letarte (The Hospital for Sick Children, Toronto, Canada) and Jose Miguel Lopez Novoa (Universidad de Salamanca, Salamanca, Spain) for kindly providing the *Eng* haploinsufficient strain.

### Funding

This work was supported by grants from Ministerio de Economía y Competitividad of Spain (RTC-2014-2626-1 to J.E., SAF2013-46183-R to M.Q., and SAF2013-43421-R to C.B.), Comunidad de Madrid (S2010/BMD-2359, SkinModel to J.E. and M.Q.), Instituto de Salud Carlos III (PI15/01458 to J.E.), and Centro de Investigación Biomédica en Red de Enfermedades Raras (CIBERER; ISCIII-CB06/07/0038 to C.B.) financed jointly by the European Regional Development Funds (FEDER). E.C. and M.I.C. were supported by Spanish MECD-FPU and UAM-FPI fellowships, respectively.

**Conflict of interest:** none declared.

### References

- Ahmed, M.I., Mardaryev, A.N., Lewis, C.J., et al. (2011). MicroRNA-21 is an important downstream component of BMP signalling in epidermal keratinocytes. *J. Cell Sci.* **124**, 3399–3404.
- Baik, J., Magli, A., Tahara, N., et al. (2016). Endoglin integrates BMP and Wnt signalling to induce haematopoiesis through JDP2. *Nat. Commun.* **7**, 13101.
- Blitz, I.L., and Cho, K.W.Y. (2009). Finding partners: how BMPs select their targets. *Dev. Dyn.* **238**, 1321–1331.
- Botella, L.M., Sánchez-Elsner, T., Rius, C., et al. (2001). Identification of a critical Sp1 site within the endoglin promoter and its involvement in the transforming growth factor- $\beta$  stimulation. *J. Biol. Chem.* **276**, 34486–34494.
- Botella, L.M., Sánchez-Elsner, T., Sanz-Rodríguez, F., et al. (2002). Transcriptional activation of endoglin and transforming growth factor- $\beta$  signaling components by cooperative interaction between Sp1 and KLF6: their potential role in the response to vascular injury. *Blood* **100**, 4001–4010.
- Bourdeau, A., Dumont, D.J., and Letarte, M. (1999). A murine model of hereditary hemorrhagic telangiectasia. *J. Clin. Invest.* **104**, 1343–1351.
- Braun, K.M., Niemann, C., Jensen, U.B., et al. (2003). Manipulation of stem cell proliferation and lineage commitment: visualisation of label-retaining cells in wholemounts of mouse epidermis. *Development* **130**, 5241–5255.
- Cambray, S., Arber, C., Little, G., et al. (2012). Activin induces cortical interneuron identity and differentiation in embryonic stem cell-derived telencephalic neural precursors. *Nat. Commun.* **3**, 841.
- Carrasco, E., Calvo, M.I., Blázquez-Castro, A., et al. (2015). Photoactivation of ROS production in situ transiently activates cell proliferation in mouse skin and in the hair follicle stem cell niche promoting hair growth and wound healing. *J. Invest. Dermatol.* **135**, 2611–2622.
- Chase, H.B. (1954). Growth of the hair. *Physiol. Rev.* **34**, 113–126.
- Cheifetz, S., Bellón, T., Calés, C., et al. (1992). Endoglin is a component of the transforming growth factor- $\beta$  receptor system in human endothelial cells. *J. Biol. Chem.* **267**, 19027–19030.
- Cotsarelis, G., Sun, T.T., and Lavker, R.M. (1990). Label-retaining cells reside in the bulge area of pilosebaceous unit: implications for follicular stem cells, hair cycle, and skin carcinogenesis. *Cell* **61**, 1329–1337.
- Espada, J., Peinado, H., Esteller, M., et al. (2005). Direct metabolic regulation of  $\beta$ -catenin activity by the p85 $\alpha$  regulatory subunit of phosphoinositide 3-OH kinase. *Exp. Cell Res.* **305**, 409–417.
- Espada, J., Pérez-Moreno, M., Braga, V.M.M., et al. (1999). H-Ras activation promotes cytoplasmic accumulation and phosphoinositide 3-OH kinase association of  $\beta$ -catenin in epidermal keratinocytes. *J. Cell Biol.* **146**, 967–980.
- Espada, J., Varela, I., Flores, I., et al. (2008). Nuclear envelope defects cause stem cell dysfunction in premature-aging mice. *J. Cell Biol.* **181**, 27–35.
- Fischer, S.M., Baldwin, J.K., and Adams, L.M. (1986). Effects of anti-promoters and strain of mouse on tumor promoter-induced oxidants in murine epidermal cells. *Carcinogenesis* **7**, 915–918.
- Foitzik, K., LINDNER, G., MUELLER-ROEVER, S., et al. (2000). Control of murine hair follicle regression (catagen) by TGF- $\beta$ 1 in vivo. *FASEB J.* **14**, 752–760.
- Fuchs, E. (2007). Scratching the surface of skin development. *Nature* **445**, 834–842.
- Fürstenberger, G., and Marks, F. (1980). Early prostaglandin E synthesis is an obligatory event in the induction of cell proliferation in mouse epidermis in vivo by the phorbol ester TPA. *Biochem. Biophys. Res. Commun.* **92**, 749–756.
- Genander, M., Cook, P.J., Ramsköld, D., et al. (2014). BMP signaling and its pSMAD1/5 target genes differentially regulate hair follicle stem cell lineages. *Cell Stem Cell* **15**, 619–633.
- Greco, V., Chen, T., Rendl, M., et al. (2009). A two-step mechanism for stem cell activation during hair regeneration. *Cell Stem Cell* **4**, 155–169.
- He, X.C., Zhang, J., Tong, W.G., et al. (2004). BMP signaling inhibits intestinal stem cell self-renewal through suppression of Wnt- $\beta$ -catenin signaling. *Nat. Genet.* **36**, 1117–1121.
- Heldin, C.H., Miyazono, K., and ten Dijke, P. (1997). TGF- $\beta$  signalling from cell membrane to nucleus through SMAD proteins. *Nature* **390**, 465–471.
- Hsu, Y.-C., Li, L., and Fuchs, E. (2014). Emerging interactions between skin stem cells and their niches. *Nat. Med.* **20**, 847–856.
- Kang, Y., He, W., Tulley, S., et al. (2005). Breast cancer bone metastasis mediated by the Smad tumor suppressor pathway. *Proc. Natl Acad. Sci. USA* **102**, 13909–13914.
- Kapur, N., Morine, K., and Letarte, M. (2013). Endoglin: a critical mediator of cardiovascular health. *Vasc. Health Risk Manag.* **9**, 195–206.
- Kobielak, K., Stokes, N., de la Cruz, J., et al. (2007). Loss of a quiescent niche but not follicle stem cells in the absence of bone morphogenetic protein signaling. *Proc. Natl Acad. Sci. USA* **104**, 10063–10068.
- Kühl, S.J., and Kühl, M. (2013). On the role of Wnt/ $\beta$ -catenin signaling in stem cells. *Biochim. Biophys. Acta Gen. Subj.* **1830**, 2297–2306.
- Lebrin, F., Goumans, M.J., Jonker, L., et al. (2004). Endoglin promotes endothelial cell proliferation and TGF- $\beta$ /ALK1 signal transduction. *EMBO J.* **23**, 4018–4028.
- Lin, H.-Y., and Yang, L.-T. (2013). Differential response of epithelial stem cell populations in hair follicles to TGF- $\beta$  signaling. *Dev. Biol.* **373**, 394–406.
- López-Novoa, J.M., and Bernabeu, C. (2010). The physiological role of endoglin in the cardiovascular system. *Am. J. Physiol. Heart Circ. Physiol.* **299**, H959–H974.
- McAllister, K.A., Grogg, K.M., Johnson, D.W., et al. (1994). Endoglin, a TGF- $\beta$  binding protein of endothelial cells, is the gene for hereditary haemorrhagic telangiectasia type 1. *Nat. Genet.* **8**, 345–351.

- Morin, P.J. (1997). Activation of  $\beta$ -catenin-Tcf signaling in colon cancer by mutations in  $\beta$ -catenin or APC. *Science* 275, 1787–1790.
- Morris, R.J., Liu, Y., Marles, L., et al. (2004). Capturing and profiling adult hair follicle stem cells. *Nat. Biotechnol.* 22, 411–417.
- Müller-Röver, S., Foitzik, K., Paus, R., et al. (2001). A comprehensive guide for the accurate classification of murine hair follicles in distinct hair cycle stages. *J. Invest. Dermatol.* 117, 3–15.
- Oshimori, N., and Fuchs, E. (2012). Paracrine TGF- $\beta$  signaling counterbalances BMP-mediated repression in hair follicle stem cell activation. *Cell Stem Cell* 10, 63–75.
- Paus, R., Müller-Röver, S., Van Der Veen, C., et al. (1999). A comprehensive guide for the recognition and classification of distinct stages of hair follicle morphogenesis. *J. Invest. Dermatol.* 113, 523–532.
- Perez-Gomez, E., Villa-Morales, M., Santos, J., et al. (2007). A role for endoglin as a suppressor of malignancy during mouse skin carcinogenesis. *Cancer Res.* 67, 10268–10277.
- Plikus, M.V. (2009). Analyses of regenerative wave patterns in adult hair follicle populations reveal macro-environmental regulation of stem cell activity. *Int. J. Dev. Biol.* 53, 857–868.
- Plikus, M.V., Baker, R.E., Chen, C.C., et al. (2011). Self-organizing and stochastic behaviors during the regeneration of hair stem cells. *Science* 332, 586–589.
- Plikus, M.V., and Chuong, C.-M. (2008). Complex hair cycle domain patterns and regenerative hair waves in living rodents. *J. Invest. Dermatol.* 128, 1071–1080.
- Plikus, M.V., Mayer, J.A., de la Cruz, D., et al. (2008). Cyclic dermal BMP signalling regulates stem cell activation during hair regeneration. *Nature* 451, 340–344.
- Pérez-Gómez, E., Jerkic, M., Prieto, M., et al. (2014). Impaired wound repair in adult endoglin heterozygous mice associated with lower NO bioavailability. *J. Invest. Dermatol.* 134, 247–255.
- Quintanilla, M., Ramirez, J.R., Pérez-Gómez, E., et al. (2003). Expression of the TGF- $\beta$  coreceptor endoglin in epidermal keratinocytes and its dual role in multistage mouse skin carcinogenesis. *Oncogene* 22, 5976–5985.
- Rendl, M., Polak, L., and Fuchs, E. (2008). BMP signaling in dermal papilla cells is required for their hair follicle-inductive properties. *Genes Dev.* 22, 543–557.
- Rompolas, P., Mesa, K.R., and Greco, V. (2013). Spatial organization within a niche as a determinant of stem-cell fate. *Nature* 502, 513–518.
- Sanz-Rodríguez, F., Guerrero-Esteo, M., Botella, L.M., et al. (2004). Endoglin regulates cytoskeletal organization through binding to ZRP-1, a member of the LIM family of proteins. *J. Biol. Chem.* 279, 32858–32868.
- Sasai, Y. (2013). Cytosystems dynamics in self-organization of tissue architecture. *Nature* 493, 318–326.
- Schneider, M.R., Schmidt-Ullrich, R., and Paus, R. (2009). The hair follicle as a dynamic miniorgan. *Curr. Biol.* 19, R132–R142.
- Shi, Y., and Massagué, J. (2003). Mechanisms of TGF- $\beta$  signaling from cell membrane to the nucleus. *Cell* 113, 685–700.
- Shimomura, Y., and Christiano, A.M. (2010). Biology and genetics of hair. *Annu. Rev. Genomics Hum. Genet.* 11, 109–132.
- Smith, A.G. (1991). Culture and differentiation of embryonic stem cells. *J. Tissue Cult. Methods* 13, 89–94.
- Sun, T.T., Costasarelis, G., and Lavker, R.M. (1991). Hair follicular stem cells: the bulge-activation hypothesis. *J. Invest. Dermatol.* 96, S77–S78.
- Takao, Y., Yokota, T., and Koide, H. (2007).  $\beta$ -catenin up-regulates Nanog expression through interaction with Oct-3/4 in embryonic stem cells. *Biochem. Biophys. Res. Commun.* 353, 699–705.
- Tasseff, R., Bheda-Malge, A., DiColandrea, T., et al. (2014). Mouse hair cycle expression dynamics modeled as coupled mesenchymal and epithelial oscillators. *PLoS Comput. Biol.* 10, e1003914.
- Tumbar, T., Guasch, G., Greco, V., et al. (2004). Defining the epithelial stem cell niche in skin. *Science* 303, 359–363.